

Reorganization of Ternary Lipid Mixtures of Non-Phosphorylated Phosphatidylinositol Interacting with Angiomotin

*Ann C. Kimble-Hill^{*a}, Horia I. Petrache^b, Soenke Seifert^c, and Millicent A. Firestone^d*

^aDepartment of Biochemistry and Molecular Biology, Indiana University School of Medicine, MS 4053, 635 Barnhill Dr., Indianapolis, IN 46202; ^b Department of Physics, Indiana University Purdue University Indianapolis, LD 154, 402 N. Blackford St., Indianapolis, IN 46202; ^c X-Ray Science Division, Advanced Photon Source, Argonne National Laboratory, Argonne, IL 60439;

^dCenter for Integrated Nanotechnologies, Los Alamos National Laboratory, MPA-CINT, MS K771, Los Alamos, NM 87545.

^{*}To whom correspondence should be addressed. Email: ankimble@umail.iu.edu. Tel: +1-317-278-1763.

This is the author's manuscript of the article published in final edited form as:

Kimble-Hill, A. C., Petrache, H. I., Seifert, S., & Firestone, M. A. (2018). Reorganization of Ternary Lipid Mixtures of Non-Phosphorylated Phosphatidylinositol Interacting with Angiomotin. *The Journal of Physical Chemistry B*. <https://doi.org/10.1021/acs.jpcb.7b12641>

1
2
3 ABSTRACT. Phosphatidylinositol (PI) lipids are necessary for many cellular signaling pathways
4
5 of membrane associated proteins, such as Angiomotin (Amot). The Amot family regulates cellular
6
7 polarity, growth, and migration. Given the low concentration of PI lipids in these membranes, it is
8
9 likely that such protein-membrane interactions are stabilized by lipid domains or small lipid
10
11 clusters. By small-angle x-ray scattering, we show that non-phosphorylated PI lipids induce lipid
12
13 de-mixing in ternary mixtures of phosphatidylcholine (PC) and phosphatidylethanolamine (PE),
14
15 likely due to preferential interactions between the head groups of PE and PI. These results were
16
17 obtained in the presence of buffer containing concentrations of Tris, HEPES, NaCl, EDTA, DTT,
18
19 and Benzamidine at pH 8.0 that in previous work showed an ability to cause PC to phase separate
20
21 but are necessary to stabilize Amot for in vitro experimentation. Collectively, this provided a
22
23 framework for determining the effect of Amot on lipid organization. Using fluorescence
24
25 spectroscopy, we were able to show that the association of Amot with this lipid platform causes
26
27 significant reorganization of the lipid into a more homogenous organization. This reorganization
28
29 mechanism could be the basis for Amot membrane association and fusigenic activity previously
30
31 described in the literature and should be taken into consideration in future protein-membrane
32
33 interaction studies.
34
35
36
37
38
39
40
41
42
43
44
45
46
47
48
49
50
51
52
53
54
55
56
57
58
59
60

Introduction

Angiomotins (Amot) are a family of proteins shown to regulate transcription and cellular organization¹. The Amot coiled-coil homology (ACCH) domain directs this protein to membranes via a specific affinity for selected phosphatidylinositol (PI). PIs are a family of negatively charged glycerophospholipids with an inositol ring that can be phosphorylated at the 3', 4', and 5' positions and play an important role in several biological signaling events^{2, 3}. Although considerable attention has been focused on phosphorylated PIs, several recent reports describe key biological functions/roles in inducing disease states played by non-phosphorylated lipids^{4, 5}. Non-phosphorylated PI (Figure 1) is a negatively charged, naturally occurring lipid found in a variety of biological membranes that participate in scaffolding, cellular compartmentalization, and signal transduction^{6, 7, 8}.

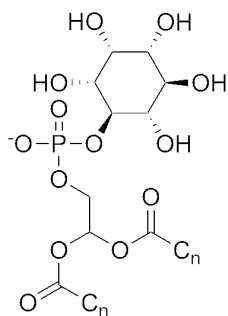


Figure 1. Pictorial representations of phosphatidylinositol (PI)

When PI is selectively phosphorylated by enzymes, it forms three mono-phosphorylated PI (PIP) family members: phosphatidylinositol 3-phosphate (PI3P), phosphatidylinositol 4-phosphate (PI4P), and phosphatidylinositol 5-phosphate (PI5P). PI3P, which is phosphorylated at the 3' position on the inositol ring (Figure 2), is generally found in apical membranes and microdomains of early endosomes and has been determined to play a role in membrane/vesicle trafficking, and receptor internalization in metabolism and anti-apoptosis^{9, 10, 11, 12, 13, 14, 15}. Likewise, PI4P is found

1
2
3 in membrane invaginations and endosomes^{16, 17} and participates in the preliminary steps of
4 neurotransmitter exocytosis of dense-core vesicles^{18, 19, 20}. Lastly, PI5P is found in low
5 concentration in the plasma membrane and is a major regulator of F-actin organization and GLUT4
6 translocation²¹. Lastly, PI5P is found in low concentration in the plasma membrane and is a major
7 regulator of F-actin organization and GLUT4 translocation²¹.
8
9

10
11
12 PIPs can undergo the same selective enzymatic phosphorylation to form the di-phosphorylated
13 PIs (PIP2) family members. Phosphatidylinositol 3,5-bisphosphate (PI3,5P2), generally the
14 product of 3' phosphorylation of PI5P, is not very abundant in cells and plays a role in insulin
15 related GLUT4 translocation²². Phosphatidylinositol 3,4,-bisphosphate (PI3,4P2) plays a role in
16 regulating micropinocytosis, endocytosis, membrane ruffling, focal adhesions, and the maturation
17 of clathrin-coated pits for endocytosis^{23, 24, 25}. Phosphatidylinositol 4,5-bisphosphate (PI4,5P2) is
18 the most abundant of endogenously expressed phosphorylated PIs²⁶, and is essential in the
19 regulation of membrane trafficking to maintain cellular polarity^{18, 27, 28, 29, 30, 31}. PI4,5P2 can be
20 phosphorylated at the 3' position to form the last member of the PI family, phosphatidylinositol
21 3,4,5-trisphosphate (PI3,4,5P3 or PIP3). PIP3 has been linked to maintaining cell membrane
22 polarization, as these lipids have been shown to phase separate to the basolateral membrane, a key
23 hallmark for the establishment of cell-cell and cell-extracellular matrix contacts^{32, 33, 34, 35}.
24
25
26
27
28
29
30
31
32
33
34
35
36
37
38
39
40
41
42
43
44
45
46
47
48
49
50
51
52
53
54
55
56
57
58
59
60

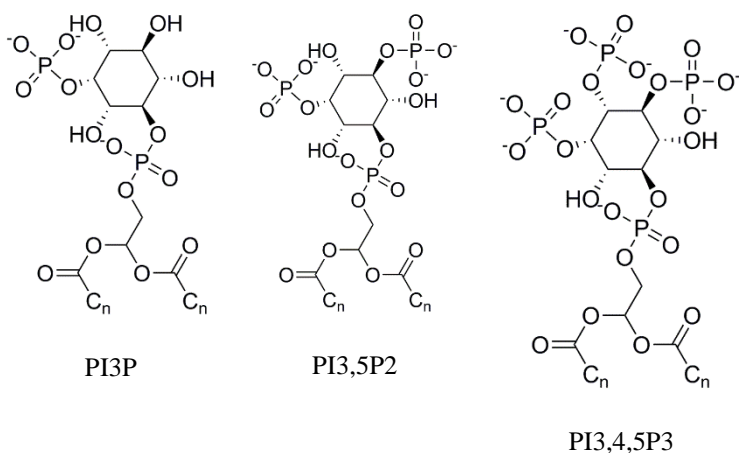


Figure 2. Pictorial representations of mono-phosphorylated PI (PIP) at the 3' position on the inositol ring (can also occur at the 4' and 5' position), di-phosphorylated PIP2, and tri-phosphorylated PIP3.

While the varying levels of PI phosphorylation has been linked to maintaining cellular polarity and organization, the expression level of selected PI family members has been linked to the selective affinity and activity of the ACCH domain. The ACCH domain has a modest affinity for non-phosphorylated PI, highest affinity is for mono-phosphorylated PIs, and no appreciable affinity to di- and tri-phosphorylated PIs^{36, 37, 38, 39}. After associating with membranes containing PIs, the ACCH domain then exhibits vesicle joining, membrane remodeling, and membrane protein recycling activity^{36, 40}. Additionally, several other membrane associated domains that have a high affinity for PIPs also show a modest affinity for non-phosphorylated PIs⁴¹. Collectively, this suggests that protein affinity to lipid platforms possessing either non- or mono-phosphorylated PIs depend on the nature of the lipid surfaces, not necessarily specific to the degree of phosphorylation but rather the interaction of PI head groups with other lipids^{42, 43, 44, 45}. This is particularly valid given the ACCH domain inability to discriminate between di- and tri-phosphorylated PIs³⁶. Therefore, we endeavored to determine the mechanism(s) that drive this selective affinity, including the events leading to phase separation.

Traditionally, the appearance of lipid phase separations is described as being a function of acyl chain fluidity, cholesterol miscibility, and environment effects on the lipids^{46, 47}. Few reports, however, have suggested that charge is a major driver in phase separation. For example, work reported by Gordon *et al.* characterized domain formation in binary mixtures of phosphatidylserine (PS)-phosphatidylcholine (PC) as differing from those of phosphatidylethanolamine (PE)-PC⁴⁸. Ternary mixtures of phosphatidylglycerol (PG)-PC-cholesterol and PS-PC-cholesterol have been reported to form domains that were regulated by membrane charging^{49, 50}.

Several studies have examined the structure of two-component mixtures of PC and phosphorylated PIs to ascertain the lipid platform or presence of phase separation that causes protein affinities for phosphatidylinositol lipids. It has been reported that PIP and PIP2 in PC mixtures have pH-dependent phase separations driven by positively charged solutes that stabilize hydrogen bonding between hydroxyl groups and phosphoryl groups on the PI lipid^{26, 51, 52, 53}. However, work done with unsaturated acyl chains in PCs has not been as clear. Conflicting literature reported that the degree of unsaturation and length of the acyl chains, as well as the position and amount of PI phosphorylation, led to varied ability for demixing^{54, 55, 56}. Binary mixtures with these lipids are a complicated story that involves both inter- and intra-molecular hydrogen bonding⁵⁶. In the presence of PC, non-phosphorylated PI appeared to require the presence of di-phosphorylated PIP2s to de-mix, as the clustering was suggested to be a result of enhanced PI phosphomonoester ionization^{53, 57}. Furthermore, Graber *et al.* reported that ternary mixtures including PE lead to hydrogen bonding between the primary amine of the PE and the PIP 3'- or 5'-phosphomonoester groups, without the appearance of phase separation^{57, 58}. While it is clear that phase separation occurs in PC/PIP mixtures, even as low as 3% PIP⁵², it is not clear if Amot senses a phase separation in the non-phosphorylated mixture. However, based on the lipid

1
2
3 affinity assays conducted by Heller et al., it was determined that the ACCH domain had a strong
4
5 affinity for PI and PIP, and almost none for PIP2 and PIP3 containing mixtures. It is clear that this
6
7 PC-PE-non-phosphorylated PI mixture must have similar structures to those with PC-PIP
8
9 liposomes³⁶.

10
11
12 The literature has little indication that ternary PC/PE/PI mixtures have phase separations^{50, 59},
13
14 however the presence of PI lipids plays a key role in deformation of liposomes based on electron
15
16 micrographs obtained by Heller et al.³⁶. Although there has not been a previous report with detailed
17
18 analysis of the structures that these mixtures may form within the membrane as a signaling
19
20 platform, we hypothesized that the incorporation of PE into this lipid mixture will cause
21
22 intramolecular hydrogen bonding with the inositol head group of the non-phosphorylated PI, in a
23
24 manner similar to that seen in PC/PIP mixtures, where the PIPs increased ionization state of the
25
26 phosphomonoester group is maintained by a higher pH buffer. In this report, we show that
27
28 increasing the non-phosphorylated PI lipid content generates a coexistence of lipid phases as seen
29
30 by small-angle x-ray scattering of multi-lamellar lipid vesicles (MLVs). We infer that this phase
31
32 separation tendency of these lipid platforms is a factor in Amot affinity. Fluorescence quenching
33
34 is then used to show that the affinity of the ACCH domain to non-phosphorylated PI containing
35
36 liposomes is correlated to the formation of PI-induced domains and that this interaction causes
37
38 further lipid reorganization. As a result, we suggest the need for further investigation into the
39
40 hydrogen bonding that occurs between PE and non-phosphorylated PI leading to this de-mixing
41
42 behavior and potential implications on other physical parameters such as membrane curvature.
43
44
45
46
47
48

49 **Experimental Methods**

50
51 *Materials.* 1-palmitoyl-2-oleoyl-*sn*-glycero-3-phosphatidylcholine (POPC), 1-palmitoyl-2-
52
53 oleoyl-*sn*-glycero-3-phosphatidylethanolamine (POPE), soy L- α -phosphatidylinositol (PI), 1-
54
55
56
57
58
59
60

oleoyl-2-(6-((4,4-difluoro-1,3-dimethyl-5-(4-methoxyphenyl)-4-bora-3a,4a-diaza-s-indacene-2-propionyl)amino)hexanoyl)-*sn*-glycero-3-phosphoinositol (TopFluor TMR PI), 1-oleoyl-2-(6-((4,4-difluoro-1,3-dimethyl-5-(4-methoxyphenyl)-4-bora-3a,4a-diaza-s-indacene-2-propionyl)amino)hexanoyl)-*sn*-glycero-3-phosphatidylethanolamine (TopFluor TMR PE), and 1-palmitoyl-2-{12-[(7-nitro-2-1,3-benzoxadiazol-4-yl)amino]dodecanoyl}-*sn*-glycero-3-phosphatidylcholine (NBD PC) were purchased from Avanti Polar Lipids (Alabaster, AL). Buffer components tris(hydroxymethyl)aminomethane (Tris), 4-(2-hydroxyethyl)-1-piperazineethanesulfonic acid (HEPES), sodium chloride, ethylenediaminetetraacetic acid (EDTA), dithiothreitol (DTT), and benzamidine were purchased from Fisher Scientific (Pittsburgh, PA). Dodecyl thiomaltopyranoside was purchased from Anatrace (Maumee, OH). The buffer solution used for all experiments contained 50 mM Tris, 600 mM HEPES, 300 mM NaCl, 0.5 mM EDTA, 1 mM DTT, 4 mM Benzamidine, and 24.7 μ M dodecyl thiomaltopyranoside (pH 8.0) (referred to as Amot ACCH domain elution buffer).

Methodology

Protein Purification. The Amot ACCH domain cDNA was subcloned into the pGEX expression plasmid and transformed into *Escherichia coli* BL21 (DE3) cells as previously described⁶⁰. Mutations in the DNA sequence were cloned into the vector using Pfu Polymerase AD in a site directed mutagenesis polymerase chain reaction^{61, 62, 63}. Cells were grown in 2xTY medium with 100 mg/L ampicillin at 37°C. 0.1mM isopropyl-beta-D-thiogalactopyranoside was used to induce protein synthesis at 16°C overnight. Cells were pelleted by centrifugation and solubilized in lysis buffer (phosphate buffered saline solution containing 1 mM DTT, 4 mM Benzamidine, and 24.7 μ M dodecyl thiomaltopyranoside). 50g/L lysozyme was used to lyse the cells using previously described methodology⁶⁴. Lysate was then collected by centrifugation at 15000 rpm at 4°C for 30

minutes using a JA-10 rotor. Protein was purified using batch purification of glutathione resin⁶⁵,
⁶⁶, ⁶⁷. The protein was eluted from the resin by 50mM glutathione added to an elution buffer
containing 50 mM Tris, 600 mM HEPES, 300 mM NaCl, 0.5 mM EDTA, 1 mM DTT, 4 mM
Benzamidine, 24.7 μ M dodecyl thiomaltopyranoside. High salts and detergents were included in
the elution buffer to increase protein stability in solution at concentrations $> 0.5\text{g/L}$ (10 μ M). The
proteins were analyzed for purity using SDS-PAGE and concentrated using a 10 kDa filter tube to
 $\geq 32\mu\text{M}$ for storage.

Liposome Formation. Multi-lamellar vesicles (MLVs) were prepared using previously
described methods^{68, 69, 70}. In short, MLVs were prepared by hydrating lyophilized lipid powder in
1 to 6 mL aqueous solution to make a final lipid concentration of 100 mM. To ensure complete
mixing, solutions were heated above 90°C for an hour, put through 3-freeze/thaw cycles, and then
bath sonicated for over an hour on an ice bath. Aliquots of lipid solutions were diluted to the
appropriate concentration for the specific experiment. Then the lipid mixture was equilibrated at
4°C overnight to maintain smaller vesicle sizes typically used for protein related studies⁷¹. Proteo-
liposomes were made by introducing protein to liposomes that had been sonicated at 10 mM until
there was a lack of MLV related turbidity^{72, 73}, diluting sample to concentrations as designated,
and equilibrating at 4°C overnight.

Small Angle X-ray Scattering (SAXS). Measurements were performed at the Advanced Photon
Source (APS/ANL) beamline 12-ID-C. The pinhole setup at 12-ID-C used a photon energy of 12
keV and a custom-built 4-quadrant mosaic X-ray CCD camera Platinum detector (1024x1024
pixel). The sample-to-detector distance was $\sim 2.2\text{m}$ and had a flux of approximately
 5×10^{12} photons/second. Samples were measured as suspended droplets for 0.1s at $\sim 23^\circ\text{C}$ for 0.1s.
2D scattering data for 5 shots were averaged and integrated over the chi angle to obtain intensity

versus q (\AA^{-1}). Scattering intensities were analyzed using Irena software developed for use in Igor⁷⁴. The Lorentzian peak, which fits intensity scattering curves using script in Igor version 6.3, was used to determine the peak position of the scattering curves that were used to calculate the lattice spacing (d -spacing) which comprises the average thickness of the membrane and the water layer⁷⁵. For lamellar structures, the d -spacing can be calculated from the position of the first order diffraction peak, $q_{0,0,1} = 2\pi/d$. For each lipid composition, scattering measurements were performed from at least 3 preparations. No significant differences in the scattering peak position(s) were observed between samples.

Fluorescence Quenching. Vesicles for these experiments contain 0.5 mol% NBD PC and 2 mol% of either TopFluor TMR lipid (PE for 0 mol% PI mixtures, and PI for all other lipid mixtures) as the donor-acceptor pair. Fluorescence measurements were taken on a black 384-well plate (Corning 3571) using a Flexstation II plate reader. NBD PC was excited using a wavelength of 460nm and the intensity of the emission was measured at 534nm. The background fluorescence of the lipids and buffer were < 1% of the samples containing fluorophores and therefore were not subtracted from the intensity of the signal. Background fluorescence from the ACCH domain was $\geq 1\%$ and were subtracted from the intensity measured from protein + lipids samples. Proteoliposomes were made by incubating 15.6 μ M protein GST-tagged Amot80/130 ACCH domain in 0.18mM of POPC/POPE/PI (80-X/20/X mol%) prepared as previously described and then incubated on an orbital shaker in the dark at room temperature overnight. The protein concentration chosen has been previously reported to be saturating for PI containing mixtures³⁶. Fluorescence measurements were then taken at 22°C, divided by the volume of the sample, and reported as a normalized intensity ($n=5$).

Results and Discussion

Lipid Small Angle X-ray Scattering.

POPC/POPE mixture. Figure 3 shows SAXS data collected on MLVs containing either pure POPC or POPE compared to an 80/20 mol% mixture of POPC/POPE. In the buffer described in the Methods, pure POPE gives two Bragg peaks with a q value of 0.11 \AA^{-1} and a temperature related peak at a q of 0.102 \AA^{-1} , as demonstrated by temperature scan measurements in Figure S2B. The scattering profiles are similar to measurements previously reported for PE membranes^{76, 77, 78}, however the presence of buffer broadens features in the scattering. The effect of buffers on POPC scattering is more pronounced than for POPE, resulting in the superposition of Bragg peaks and very broad features, as we have shown before⁷⁹. We should note that these broad features due to the choice of buffer, which is necessary for ACCH domain stability, preclude a detailed quantitative analysis of the scattering profile. We have recently reported the effect of each of the buffer components on POPC scattering behavior⁷⁹, and we have summarized these results in comparison with the current buffer in Figure S1. However, as we will show, the observed differences in scattering profiles are sufficient to allow a comparison of binary and ternary lipid mixtures in the same buffer conditions. In Figure 3, we compare the scattering of pure lipid with the 80/20 mol% POPC/POPE mixture of interest. We chose this particular mixture because Amot has been shown to have no affinity to it until PI is added³⁶. The peak positions of the 80/20 mol% POPC/POPE MLVs are more similar to that seen from pure POPC than from pure POPE with no additional peaks (Table 1). Similarity with POPC scattering indicates that POPE does not significantly affect the lamellar structure of POPC when buffers are present, while the absence of additional peaks suggests that POPE is integrated in the POPC matrix and does not separate into a different phase.

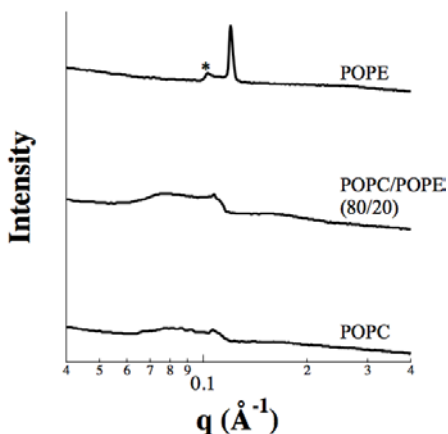


Figure 3. SAXS profiles of POPC, POPE, and POPC/POPE (80/20 mol%) samples in Amot ACCH domain elution buffer at 22°C. * denotes a temperature related Bragg peak.

Table 1. Position of diffraction peaks, $q(\text{\AA}^{-1})$, of lipid mixtures from Figure 3

Bragg Peak (\AA^{-1})	POPC	POPE	POPC/POPE (80/20 mol%)
1 st	0.085	0.102*	0.081
2 nd	0.107	0.111	0.107
3 rd	0.202	0.210	0.149

*Denotes diffraction peak for a temperature related Bragg peak.

Binary mixtures with non-phosphorylated PI. Figure 4 shows SAXS data collected on binary mixtures of POPC/PI and POPE/PI to show the effects of incorporating PI into POPC or POPE membranes. The binary mixing ratios were chosen to reflect the ternary PC/PE/PI mixing ratio of interest for Amot-membrane association. Equimolar POPE/PI MLVs diffract as 3 visible repeating Bragg peaks that decrease in intensity with increasing q values (Table 2). This diffraction pattern presents sharp peaks characteristic to POPE vesicles but with a larger q value of 0.121 \AA^{-1} (Table 2) compared to 0.110 \AA^{-1} for POPE alone (Table 1). As this equimolar mixture exhibits a single d -spacing, it suggests that PI and POPE are well mixed and form a singular phase.

Next, we compare these results with the 80/20 mol% POPC/PI MLVs diffraction profile also shown in Figure 4. The POPC/PI profile presents two large features with a small shoulder around $q \sim 0.1 \text{ \AA}^{-1}$ (Table 2). The large features appear at a q value of 0.09 and 0.18 \AA^{-1} , respectively (Table 2), which indicates these are a pair of broad repeating lamellar Bragg peaks. This scattering profile is clearly different from that of POPC alone (Figure 3) and that of the 80/20 mol% POPC/POPE mixture which is reproduced in Figure 2 for comparison. Figure 2 shows that the scattering features of POPC/PI are more pronounced than those of POPC/POPE which indicates that addition of PI to POPC in our buffer stabilizes the lamellar structure to a much larger extent than adding POPE. In particular, the low q region $\leq 0.1 \text{ \AA}^{-1}$ of POPC/PI is now narrower than that of POPC/POPE (or POPC alone for that matter) and the second order scattering for $q \leq 0.2 \text{ \AA}^{-1}$ is more pronounced (Figure 4). This sharpening of the scattering profile indicates that the presence of PI prevents some of the buffer/salt effects on POPC lamellar structure previously reported⁷⁹ and seen in Figures S2.

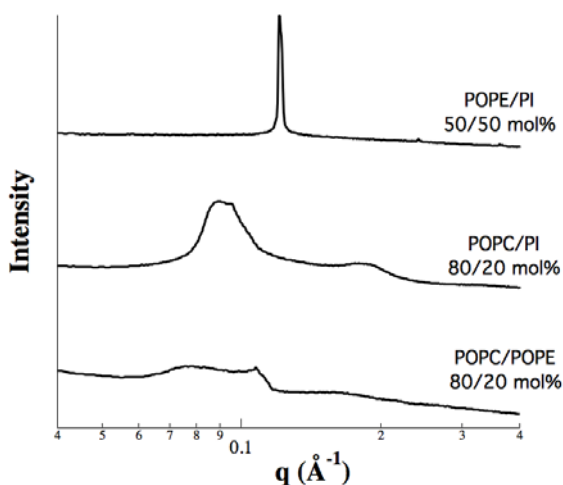


Figure 4. SAXS profiles of binary mixtures of POPC, POPE, and PI that reflect the relative ratio of those lipids in the POPC/POPE/PI (60/20/20 mol%) mixtures previously reported to recruit Amot association³⁶. All samples were made in Amot ACCH domain elution buffer at 22°C.

Table 2. Position of diffraction peaks, $q(\text{\AA}^{-1})$, of lipid mixtures from Figure 4

Bragg Peak (\AA^{-1})	POPC/POPE (80/20 mol%)	POPC/PI (80/20 mol%)	POPE/PI (50/50 mol%)
1 st	0.081	0.090	0.121
2 nd	0.107	0.095	0.242
3 rd	0.149	0.177	0.362
4 th		0.267	

Ternary mixtures of POPC-POPE-PI. Figure 5 compares the 60/20/20 mol% POPC/POPE/PI mixture with the 50/50 mol% POPE/PI and the 80/20 mol% POPC/PI binary mixtures previously discussed. The scattering pattern from the ternary mixture is a superposition of scattering features from both binary mixtures shifted to lower q values (Table 3). The diffraction pattern presents two lamellar repeat spacings, with first order peaks appearing at q values 0.08 and 0.111 \AA^{-1} , respectively. The Bragg peaks corresponding to the larger repeat spacing (smaller q) are broader, indicating a more disordered (fluid) phase similar to the POPC/PI binary mixture, while those corresponding to the smaller repeat spacing (larger q) are sharper and similar to the POPE/PI binary mixture. This indicates that the ternary mixture is not homogenous but separates into two prominent phases, one rich in POPC and the other rich in POPE/PI. One possible interpretation is that PI interacts preferentially with POPE, causing the POPE/PI complex to separate from the POPC dominant mixture. Therefore, we investigated the effect of increasing the PI concentration incorporated into POPC/POPE mixtures (Figure 6).

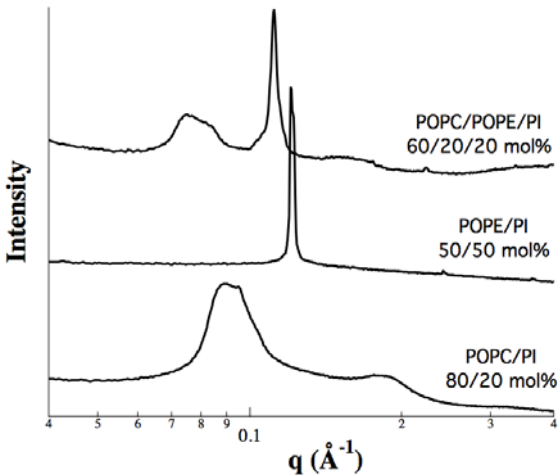


Figure 5. SAXS intensity profiles of POPC, POPE, and POPC/POPE as PI is added to the mixture. All samples were made in Amot ACCH domain elution buffer at 22°C.

Table 3. Position of diffraction peaks, $q(\text{\AA}^{-1})$, of lipid mixtures from Figure 5

Bragg Peak (\AA^{-1})	POPC/PI (80/20 mol%)	POPE/PI (50/50 mol%)	POPC/POPE/PI (60/20/20 mol%)
1 st	0.090	0.121	0.080
2 nd	0.095	0.242	0.111
3 rd	0.177	0.362	0.150
4 th	0.267		0.223

Figure 6 compares SAXS data collected on two different ternary mixtures of POPC/POPE/PI MLVs: 70/20/10 and 60/20/20 mol%. At 10 mol%, PI is less effective in separating out POPE and results in a scattering profile that overlaps with the previously mentioned POPC/POPE peak and a small shoulder peak that correlates with phases associated with POPE/PI (Table 4).

The SAXS diffraction pattern of the 3-component POPC/POPE/PI 70/20/10 and 60/20/20 mol% mixtures suggests that the interaction of two different charged lipids, that is PC-PI and/or PE-PI, alters the packing arrangement of the lipids and hence structural order of the bilayer. The profile

suggests that the lipids demix which warrants a discussion of the lipid components, both the acyl chain and head group, that could contribute to this effect.

First, we considered the complexity of the acyl chains. The PC and PE lipids in this study both have palmitoyl (16:0) and oleoyl (18:1) acyl chains. However, the naturally derived PI lipid is a mixture of 5 different lipids with varying saturated and polyunsaturated acyl chains. Several prior reports in the literature have already suggested that acyl chain composition can have a dramatic effect on the ability of PI lipids to demix from other lipids. Such an example is the work by Jiang et al. that reported porcine brain PI(4,5)P₂ had no evidence of demixing at neutral pH, in buffers not containing cations, or lipid mixtures that do not contain agents that affect membrane fluidity such as cholesterol⁵⁴. Also, the degree of PC lipid acyl chain saturation has been shown to play a role in PI ability to phase separate. Sarmiento et al. reported that mixed chain PC does not demix from 1 mol% DOPI(4)P regardless of the presence of divalent cations or the addition of previously reported saturated lipids that drive fluid/gel lipid demixing⁵⁵. The compilation of this literature suggests that the demixing seen in this report cannot simply be an effect of acyl chain mixed saturation.

Next, we considered the role of head group ionization state of PI in lipid demixing. Kooijman et al. reported lipid demixing behavior exhibited by mixed chain porcine brain PI(4,5)P₂, dioleoyl-PI(4,5)P₂ and dioleoyl-PI(3,4)P₂ in the presence of DOPC as a result of pH-dependent ionization of the head group that lent to the formation of intramolecular hydrogen bonds when incorporated into membranes as low as 1 mol%⁵⁶. Dioleoyl-PI(3,5)P₂ was not found to have the same biphasic behavior but dioleoyl-PI(3,4,5)P₃ showed a much more complicated behavior which has been described as a mixture between inter- and intra-molecular hydrogen bonding⁵⁶. This suggests that the place and degree of head group ionization has a much more complicated effect on lipid

demixing based on the ability to form complex hydrogen bonds. Later studies by Graber et al. suggested that POPC/20 mol% liver PI required the presence of porcine brain PI(4,5)P2 to demix⁵⁷, and DOPC/2mol% porcine brain PI(4,5)P2 requires the incorporation of 10 mol% plant PI in order to demix⁵³. In both instances, they suggested that the presence of mixed chain PI enhanced the 5'-phosphomonoester ionization of the PI(4,5)P2 thereby negatively charging the membrane leading to the demixing of a PI/PI(4,5)P2 complex^{53, 57}. These studies suggest that non-phosphorylated PI could indeed demix in a negatively charged membrane. The authors are unaware of work that studies buffers inducing electrostatic interactions on the surface of membranes containing non-phosphorylated PI and the consequential effect on hydroxyl groups forming hydrogen bonds with PE that may explain our results. However, previous work from this group on the buffer components on POPC⁷⁹, as well as the work provided in this report utilizing the current buffer on POPC does suggest that membrane charging could be occurring.

Furthermore, PI lipids have also been shown to demix in ternary head group mixtures. Graber et al. also included phosphatidylethanolamine (PE) into their PC-porcine brain PI(4,5)P2 mixtures and found a hydrogen bond forms between the ethanolamine head group and the PIP2 5'-phosphomonoester group without the appearance of phase separation⁵⁷. Graber et al. also reported that when PE was included with PC-PI(3,4,5)P3 mixtures there is a stepwise deprotonation of the phosphates that lends to a preference for hydrogen bonding between the primary amine of PE and the 3'-phosphate⁵⁸. The PC/PE/PI ternary mixture SAXS pattern found in this work demonstrates that the interaction of PI with PE and PC head groups is the primary interaction that determines the order and arrangement of the lipids at least at the level observed employing the scattering vector range for SAXS. However, there are no PI phosphates to interact with the PE primary amine in the mixtures of this report. In summary, the scattering profiles reported here for the PC/PE/PI

mixtures, without the presence of another negatively charged head group component, suggests that for this system the effect of the surface charge including the PE-PI head group interaction dominates the effect of chains, which is a paramount finding for the physical chemistry of lipids.

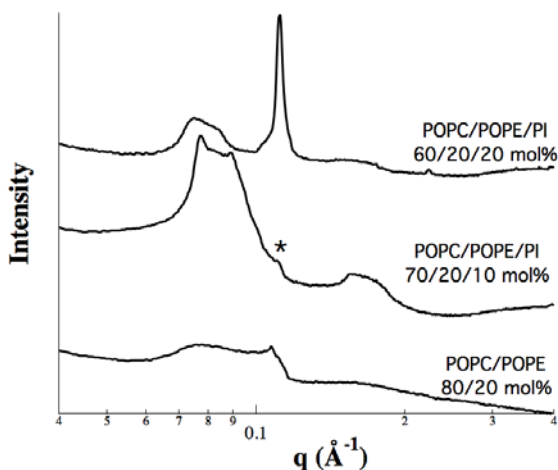


Figure 6. SAXS intensity profiles of POPC, POPE, and PI mixtures in varying ratios. All samples were made in Amot ACCH domain elution buffer at 22°C. *Denotes diffraction peak for a shoulder peak

Table 4. Position of diffraction peaks, $q(\text{\AA}^{-1})$, of lipid mixtures from Figure 6

Bragg Peak (\AA^{-1})	POPC/POPE (80/20 mol%)	POPC/POPE/PI (70/20/10 mol%)	POPC/POPE/PI (60/20/20 mol%)
1 st	0.081	0.077	0.080
2 nd	0.107	0.086	0.111
3 rd	0.149	0.095	0.150
4 th		0.111	0.223
5 th		0.158	
6 th		0.166	

Phase separation in ternary mixtures is independent of temperature. Given the complexity of the acyl chains within this ternary mixture, we studied the role of acyl chain fluidity in its phase separating behavior by looking at the scattering as a function of temperature (Figure 7). Figure 7 shows SAXS profiles of the PC/PE/PI mixture for temperature values between 1 and 41°C both under heating and cooling conditions. For comparison, we have also included the temperature scan of POPC, POPE, and POPC/20 mol% POPE, (Figure S2) which suggests a temperature dependence in PC ability to mix with PE. Although scattering peaks shift in q-values as temperature is changed, the overall scattering profile does not, except for systematic changes in peak intensities. Intensity changes are most likely due to the fact that electron densities are temperature dependent (which therefore affects the scattering form factor) and that changes in d-spacing to different q-values that are scaled by different form factors. Unlike classically studied membranes of ternary mixtures where there is phase separation between fluid and rigid lipids mediated by cholesterol content^{80, 81, 82, 83, 84, 85}, the phase separation of this POPC-POPE-PI mixture is not temperature dependent, as there are no changes in appearance of the two lipid phases as the temperature is increased above the melting temperature of all the individual components. We therefore conclude that this POPC-POPE-PI de-mixing behavior is thermostable.

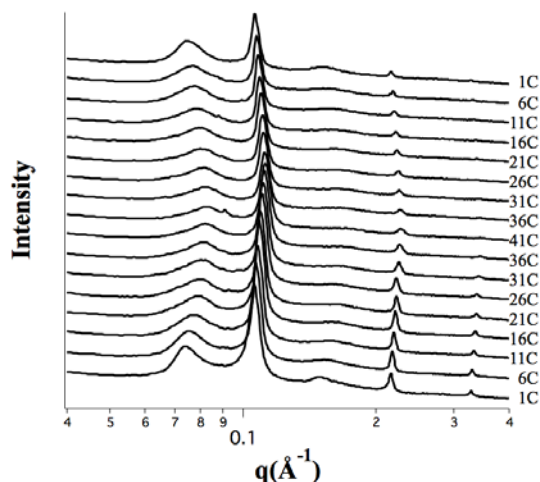


Figure 7. Temperature dependent SAXS measurements of POPC/POPE/PI (60/20/20 mol%) MLVs. MLVs from Figure 6 were equilibrated at 1°C and then slowly raised 5°C every 10 minutes up to a temperature of 41°C and then lowered at the same rate back to 1°C, where measurements were taken prior to temperature being changed.

We have shown previously that the buffer used in this study caused POPC organization to change from a characteristic d-spacing of 64 Å, a L_α phase, to a phase separating liquid phase with at least 2 d-spacings driven by the HEPES, Tris and EDTA content of the buffer⁷⁹. In that study, we suggested that the differences in the d-spacings were due to changes in the thickness of the interlamellar water space. However, in this study, the 50 mM Tris, 600 mM HEPES, 300 mM NaCl, 0.5 mM EDTA, 1 mM DTT, 4 mM Benzamidine, 24.7 μM dodecyl thiomaltopyranoside (pH 8.0) buffer had a negligible effect on the organization of POPE, only dehydrating the L_α phase by decreasing the interlamellar water space ~3 Å. The addition of 20 mol% POPE to POPC leads to a more complicated diffraction pattern than in either PC or PE alone, but it clearly indicates the presence of two phases: highly hydrated phase with a d-spacing of ~ 78 Å and a relatively dehydrated phase with a d-spacing of ~ 58 Å. While the overall diffraction is similar to that of POPC alone, the presence of POPE does affect the scattering as shown above. At the next level of

membrane complexity, the incorporation of 10 mol% PI to make a three-component mixture further complicates the scattering profile. However, comparing the scattering profiles of binary mixtures allows us to separate buffer effects from those of membrane composition. While the data presented suggest that there are interactions that led to the occurrence of phase separation in the ternary PC/PE/PI mixture leading to a phase rich in PC and another rich in PE/PI, more studies would have to be done to determine if any of the buffer components play a significant role in this result.

Lipid Fluorescence Measurements

We further examined the effect of PI on lipid organization by studying fluorescence quenching in proteo-liposomes. This method is appropriate for studies of lipid mixing and has been applied to systems in which lipid heterogeneity was introduced as a function of cholesterol content^{86, 87}, resveratrol⁸⁸, acylated cholesteryl galactoside⁸⁹, or cationic lipids⁹⁰. In this method, fluorescence quenching is maximal when donor and acceptor groups are in close proximity and it diminishes when donors and acceptors are separated in space.

Figure 8 shows data collected where NBD PC fluorescence is quenched by TopFluor TMR labeled lipids in ternary mixtures of POPC/POPE/PI vesicles (PI ranged from 0-30 mol%, POPE fraction was kept fixed at 20 mol%). The data shows that there are two different regions of NBD fluorescence behavior. In the first region, at low PI concentrations between 0-15 mol% there is a steady linear increase in NBD fluorescence from that of the PC/PE only mixture. A linear fit to this region is shown in the figure with a dashed line. The linear behavior indicates that the distribution of donor and acceptors is primarily uniform with the possibility that domains start to form towards the end of the linear regime. The second region is a plateau that occurs when PI concentration is >16 mol%, where the NBD fluorescence no longer changes as a function of %PI.

In fact, by this method, we detect a sharp decrease in fluorescence quenching as a function of %PI around 16 mol% PI which strongly suggest an abrupt reorganization of the lipid mixture at this PI concentration. Above 16 mol % PI, quenching is no longer observed, which indicates a quasi-complete separation of PI from PC. These results are consistent with SAXS measurements where two fully discrete phases were seen at ~20 mol % PI but not below, a lipid mixture that matches those previously reported to have significant Amot affinity³⁶.

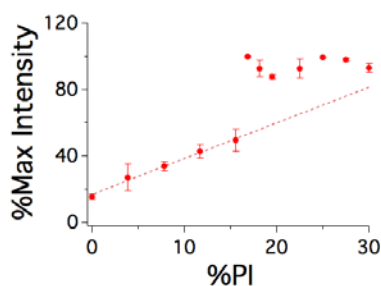


Figure 8. NBD fluorescence quenching as a function of PI concentration at room temperature. Donor was 0.5 mol % NBD PC, acceptor was 2 mol% TopFluor TMR (DOPE for 0% PI, PI for > 0% PI). Samples were liposomes containing 0.25mM of POPC/POPE/PI made at a 80-X/20/X mol% ratio. The percentage of the maximum NBD fluorescence intensity is plotted versus PI concentration as closed circles (n=5), where the linear range of the samples (dashed line) fit to a slope of ~ 2.15 ($R^2 = 0.995$).

Figure 9 shows NBD fluorescence quenching measurements using the same lipid compositions as in Figure 8 but in the presence of the Amot ACCH domain. The overall trend is similar to that of the lipid only samples, where there is a distinct linear range at low %PI followed by a plateau region. Here, however the linear region ends at ~12 mol% PI and is followed by a plateau region without a jump at higher PI concentration. Importantly, fluorescence quenching in the presence of protein persists even at high PI and is not eliminated as in the lipid only sample. This suggests

that homogeneous mixtures at low PI concentrations, behave similarly with or without protein but there is a threshold in PI concentration where the effect of protein is visibly seen. Importantly, this threshold (or critical) PI concentration is at or near the point where PI starts to induce phase separation in the ternary PC/PE/PI mixtures. Indeed, Heller et al reported that ACCH domain affinity for POPC/POPE liposomes was negligible³⁶ consistent with our measurements for samples without PI. Heller et al. reported that the ACCH domain has an appreciable affinity for POPC/POPE/PI 60/40/40 mol% liposomes. These results then show that the ACCH domain has negligible affinity for PC/PE/PI liposomes when the PI fraction is not large enough to induce lipid de-mixing and that association with these membranes inhibits the tendency for phase separation driven by the PE/PI interaction.

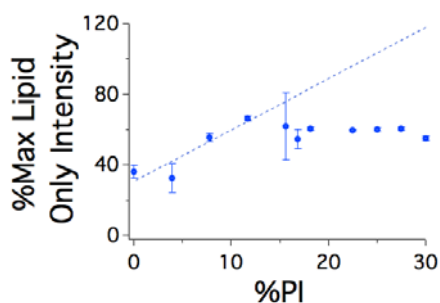


Figure 9. NBD fluorescence quenching as a function of PI concentration in the presence of the Amot ACCH domain. Donor was 0.5 mol % NBD PC, acceptor was 2 mol% TopFluor TMR (DOPE for 0% PI, PI for > 0% PI). Samples were proteo-liposomes containing 0.18mM of POPC/POPE/PI made at a 80-X/20/X mol% ratio incubated in 15.6 μ M protein. The percentage of the maximum lipid only NBD fluorescence intensity is plotted versus PI concentration as closed circles (n=5), where the linear range of the samples (dashed line) fit to a slope of ~ 2.9063 ($R^2 = 0.912$).

Generally, it is thought that the most stable lipid platform for such membrane protein signaling events would be equivalent to lipid rafts or micro-domains of phase separating lipids. Complete phase separation or domain formation in lipid mixtures is dictated by their physico-chemical characteristics, such as saturation in acyl chains or head group type⁹¹. Phase separation based on acyl chains character is not likely in this system as all of the components have similar mixed acyl chains of 16 and 18 carbons in length (Avanti reports Soy PI as being mostly made up of saturated 16 and 18 carbon chains, and unsaturated 18:1, 18:2, and 18:3 carbon chains in the natural lipid mixture while both POPC and POPE have both a saturated 16 and unsaturated 18:1 acyl chains); however, the lipid classes used in this work differ substantially on head group structure and electrical charge. The possibility of phase separation or domain formation in this case can be regarded as a consequence of local head group-head group interactions or it could be due to differences in intrinsic curvature energies of the different lipid types^{92, 93, 94, 95, 96, 97}.

Depending on the type of head group and acyl chains, phospholipids tend to induce membrane curvature^{98, 99}. These tendencies are manifested in morphological phase transition as for example in the case of DOPE which forms inverse hexagonal phases. DOPE then is said to have negative intrinsic curvature (or negative curvature tendency), while DOPC and most di-acyl chain PCs have zero or neutral curvature^{100, 101}. In contrast, PI lipids are believed to have a positive curvature tendency. Because of opposite tendencies, mixtures of these different lipid types can relieve membrane stress by packing together thereby inducing phase separation. Our results suggest the possibility that PI and PE lipids could cluster together and compensate/neutralize each other's tendency which probably confers a zero net curvature for the membrane topography while possibly presenting the head groups of that phase in a different orientation than that of the PC rich regions (Figure 10).

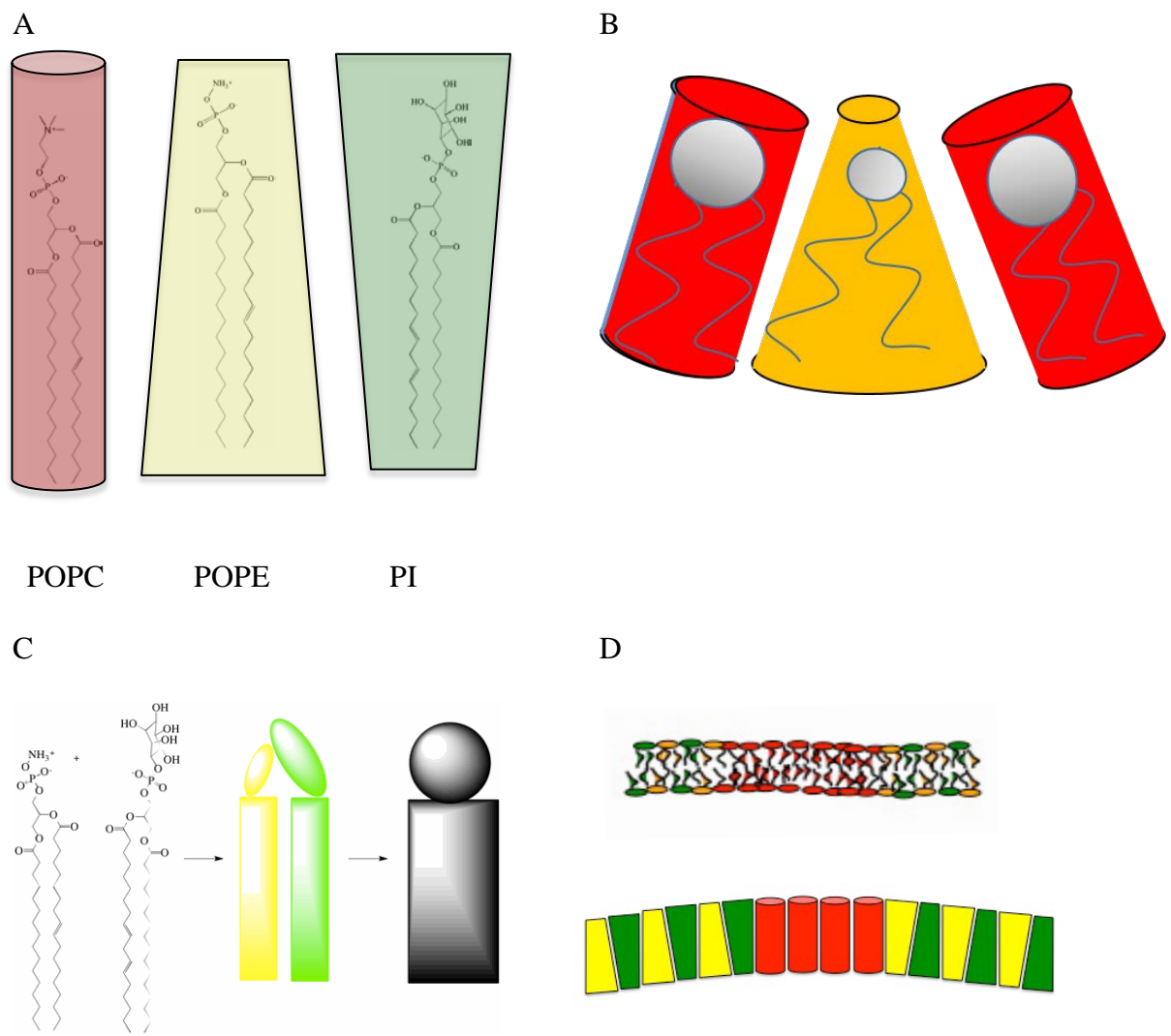


Figure 10. POPE-PI complex formation. A) Pictorial representation of the curvature tendency of each of the lipids in the mixture: cylindrical and neutral POPC (red), conical and positively charged POPE (yellow), and opposing conical and negatively charged PI (green). B) Lipids with different shapes (intrinsic curvature) may separate when mixed and cause bending of the membrane. C) The association of PI and PE lipids with opposite curvature tendencies create a net cylindrical (zero intrinsic curvature) structures which releases membrane curvature stress upon separation into domains as depicted in panel D.

Our fluorescence data indicate that these PI-induced domains in lipid bilayers are what confers the PI affinity of protein domains such as the ACCH domain to membrane surfaces. Furthermore, the incorporation of the ACCH domain can cause lipid reorganization, suggesting that the inclusion of cations and proteins capable of direct interaction with either the PE or PI head groups can affect their electrostatic interaction. One can further speculate, that the PE-PI interactions generate stable platforms necessary for vesicle fusion and budding events.

Conclusion

The objective of this study was to characterize the non-phosphorylated PI membrane that attracts proteins, such as the Amot ACCH domain, for lipid binding events. The results presented here show that PI lipids can induce lipid de-mixing in ternary lipid compositions that are not cholesterol content or temperature dependent. This behavior is most likely due to preferential interactions between PE and PI head groups. The PI-rich domains, presumably electrostatically charged by the presence of a complex buffer, are targeted by the lipid-binding ACCH domain and upon interaction leads to lipid reorganization. The experimental results in this report contribute to further understanding the mechanisms involved in Amot lipid binding and reorganization of the cellular membrane.

ASSOCIATED CONTENT

Supporting Information.

The following files are available free of charge.

Additional SAXS of lipid components in buffering agents (Figure S1) and temperature scans of 3 component mixtures (Figure S2) (PDF)

AUTHOR INFORMATION

Corresponding Author

Corresponding Author. Ann C. Kimble-Hill, § (317) 278-1763. ankimble@uemail.iu.edu

Author Contributions

The manuscript was written through contributions of all authors. ^aA.K.-H. initiated and designed the study, performed experiments, data analysis and manuscript preparation; ^dM.A.F. designed the study and data analysis; ^cS.S. acquired beam time, performed experiments and operated beam lines; ^bH.I.P. data analysis and manuscript preparation.

ACKNOWLEDGMENTS

Results shown in this report are derived from work performed at Argonne National Laboratory, X-ray Science Division at the Advanced Photon Source. Argonne was operated by UChicago Argonne, LLC, for the U.S. Department of Energy, Office of Biological and Environmental Research under contract DE-AC02-06CH11357.

Funding Sources. This work was supported, in whole or in part, by National Institutes of Health Grants K01-CA169078 (to A.K.H.) and Indiana University Collaborative Research Grants (to H.I.P.). The authors declare no competing financial interest.

ABBREVIATIONS

Angiomotin, Amot; Amot coiled-coil homology (ACCH); Ethylenediaminetetraacetic acid, EDTA; 4-(2-hydroxyethyl)-1-piperazineethanesulfonic acid, HEPES; 1-palmitoyl-2-oleoyl-*sn*-glycero-3-phosphatidylcholine, POPC; Small Angle X-ray Scattering, SAXS; 1-palmitoyl-2-oleoyl-*sn*-glycero-3-phosphatidylethanolamine (POPE), soy L- α -phosphatidylinositol (PI); tris(hydroxymethyl)aminomethane, Tris.

REFERENCES

1. Moleirinho, S.; Guerrant, W.; Kissil, J. L., The Angiomotins—from discovery to function. *FEBS letters* **2014**, 588 (16), 2693-2703.
2. Bridges, D.; Saltiel, A. R., Phosphoinositides: Key modulators of energy metabolism. *Biochimica et Biophysica Acta (BBA) - Molecular and Cell Biology of Lipids* **2015**, 1851 (6), 857-866.
3. Cauvin, C.; Echard, A., Phosphoinositides: Lipids with informative heads and mastermind functions in cell division. *Biochimica et Biophysica Acta (BBA) - Molecular and Cell Biology of Lipids* **2015**, 1851 (6), 832-843.
4. Cockcroft, S., The diverse functions of phosphatidylinositol transfer proteins. In *Current Topics in Microbiology and Immunology*, 2012; Vol. 362, pp 185-208.
5. Litvak, V.; Tian, D.; Carmon, S.; Lev, S., Nir2, a Human Homolog of Drosophila melanogaster Retinal Degeneration B Protein, Is Essential for Cytokinesis. *Molecular and Cellular Biology* **2002**, 22 (14), 5064-5075.
6. Abe, N.; Inoue, T.; Galvez, T.; Klein, L.; Meyer, T., Dissecting the role of PtdIns(4,5)P₂ in endocytosis and recycling of the transferrin receptor. *Journal of Cell Science* **2008**, 121 (9), 1488-1494.
7. Balla, T.; Szentpetery, Z.; Kim, Y. J., Phosphoinositide Signaling: New Tools and Insights. *Physiology* **2009**, 24 (4), 231-244.
8. Brown, D. A.; London, E., Functions of lipid rafts in biological membranes. *Annual Rev Cell Develop Biol* **1998**, 14 (1), 111-136.
9. Samuels, Y.; Ericson, K., Oncogenic PI3K and its role in cancer. *Current Opinion in Oncology* **2006**, 18 (1), 77-82 10.1097/01.cco.0000198021.99347.b9.
10. Engelman, J. A.; Luo, J.; Cantley, L. C., The evolution of phosphatidylinositol 3-kinases as regulators of growth and metabolism. *Nat Rev Genet* **2006**, 7 (8), 606-619.
11. Backer, J. M., The regulation and function of Class III PI3Ks: novel roles for Vps34. *Biochem J* **2008**, 410 (1), 1-17.
12. Carracedo, A.; Pandolfi, P. P., The PTEN-PI3K pathway: of feedbacks and cross-talks. *Oncogene* **2000**, 27 (41), 5527-5541.
13. Leever, S. J.; Vanhaesebroeck, B.; Waterfield, M. D., Signalling through phosphoinositide 3-kinases: the lipids take centre stage. *Current Opinion in Cell Biology* **1999**, 11 (2), 219-225.
14. Vanhaesebroeck, B.; Waterfield, M. D., Signaling by Distinct Classes of Phosphoinositide 3-Kinases. *Experimental Cell Research* **1999**, 253 (1), 239-254.
15. Fruman, D. A.; Meyers, R. E.; Cantley, L. C., PHOSPHOINOSITIDE KINASES. *Annual Review of Biochemistry* **1998**, 67 (1), 481-507.
16. Slomiany, A.; Sano, S.; Grabska, M.; Yamaki, K.; Slomiany, B. L., Gastric mucosal cell homeostatic physiome. Critical role of ER-initiated membranes restitution in the fidelity of cell function renewal. *J Physiol Pharmacol* **2004**, 55 (4), 837-860.
17. Gillooly, D. J.; Raiborg, C.; Stenmark, H., Phosphatidylinositol 3-phosphate is found in microdomains of early endosomes. *Histochemistry and Cell Biology* **2003**, 120 (6), 445-453.
18. Cremona, O.; De Camilli, P., Phosphoinositides in membrane traffic at the synapse. *Journal of Cell Science* **2001**, 114 (6), 1041-1052.
19. Osborne, S. L.; Meunier, F. A.; Schiavo, G., Phosphoinositides as Key Regulators of Synaptic Function. *Neuron* 32 (1), 9-12.

20. Wenk, M. R.; De Camilli, P., Protein-lipid interactions and phosphoinositide metabolism in membrane traffic: Insights from vesicle recycling in nerve terminals. *Proceedings of the National Academy of Sciences of the United States of America* **2004**, *101* (22), 8262-8269.
21. Sbrissa, D.; Ikononov, O. C.; Strakova, J.; Shisheva, A., Role for a Novel Signaling Intermediate, Phosphatidylinositol 5-Phosphate, in Insulin-Regulated F-Actin Stress Fiber Breakdown and GLUT4 Translocation. *Endocrinology* **2004**, *145* (11), 4853-4865.
22. Ikononov, O. C.; Sbrissa, D.; Dondapati, R.; Shisheva, A., ArPIKfyve-PIKfyve interaction and role in insulin-regulated GLUT4 translocation and glucose transport in 3T3-L1 adipocytes. *Experimental Cell Research* **2007**, *313* (11), 2404-2416.
23. Hawkins, P. T.; Stephens, L. R., Emerging evidence of signalling roles for PI(3,4)P₂ in Class I and II PI3K-regulated pathways. *Biochemical Society Transactions* **2016**, *44* (1), 307-314.
24. Hasegawa, J.; Tokuda, E.; Tenno, T.; Tsujita, K.; Sawai, H.; Hiroaki, H.; Takenawa, T.; Itoh, T., SH3YL1 regulates dorsal ruffle formation by a novel phosphoinositide-binding domain. *The Journal of Cell Biology* **2011**, *193* (5), 901-916.
25. Miki, F.; Takeshi, I.; Tadaomi, T., PI(3,4)P₂ plays critical roles in the regulation of focal adhesion dynamics of MDA-MB-231 breast cancer cells. *Cancer Science* **2017**, *108* (5), 941-951.
26. Wang, Y.-H.; Collins, A.; Guo, L.; Smith-Dupont, K. B.; Gai, F.; Svitkina, T.; Janmey, P. A., Divalent Cation-Induced Cluster Formation by Polyphosphoinositides in Model Membranes. *Journal of the American Chemical Society* **2012**, *134* (7), 3387-3395.
27. Wang, Y. J.; Wang, J.; Sun, H. Q.; Martinez, M.; Sun, Y. X.; Macia, E.; Kirchhausen, T.; Albanesi, J. P.; Roth, M. G.; Yin, H. L., Phosphatidylinositol 4 phosphate regulates targeting of clathrin adaptor AP-1 complexes to the Golgi. *Cell* **2003**, *114* (3), 299-310.
28. Brown, F. D.; Rozelle, A. L.; Yin, H. L.; Balla, T.; Donaldson, J. G., Phosphatidylinositol 4,5-bisphosphate and Arf6-regulated membrane traffic. *The Journal of Cell Biology* **2001**, *154* (5), 1007-1018.
29. Rozelle, A. L.; Machesky, L. M.; Yamamoto, M.; Driessens, M. H. E.; Insall, R. H.; Roth, M. G.; Luby-Phelps, K.; Marriott, G.; Hall, A.; Yin, H. L., Phosphatidylinositol 4,5-bisphosphate induces actin-based movement of raft-enriched vesicles through WASP-Arp2/3. *Current Biology* **2000**, *10* (6), 311-320.
30. De Matteis, M. A.; Godi, A.; Corda, D., Phosphoinositides and the Golgi complex. *Current Opinion in Cell Biology* **2002**, *14* (4), 434-447.
31. Cockcroft, S.; De Matteis, M. A., Inositol lipids as spatial regulators of membrane traffic. *Journal of Membrane Biology* **2001**, *180* (3), 187-194.
32. Martin-Belmonte, F.; Mostov, K., Phosphoinositides Control Epithelial Development. *Cell Cycle* **2007**, *6* (16), 1957-1961.
33. Gassama-Diagne, A.; Yu, W.; ter Beest, M.; Martin-Belmonte, F.; Kierbel, A.; Engel, J.; Mostov, K., Phosphatidylinositol-3,4,5-trisphosphate regulates the formation of the basolateral plasma membrane in epithelial cells. *Nature Cell Biology* **2006**, *8* (9), 963-970.
34. Martin-Belmonte, F.; Gassama, A.; Datta, A.; Yu, W.; Rescher, U.; Gerke, V.; Mostov, K., PTEN-Mediated Apical Segregation of Phosphoinositides Controls Epithelial Morphogenesis through Cdc42. *Cell* **2007**, *128* (2), 383-397.
35. Giepmans, B. N. G.; van Ijzendoorn, S. C. D., Epithelial cell-cell junctions and plasma membrane domains. *Biochimica et Biophysica Acta (BBA) - Biomembranes* **2009**, *1788* (4), 820-831.

36. Heller, B.; Adu-Gyamfi, E.; Smith-Kinnaman, W.; Babbey, C.; Vora, M.; Xue, Y.; Bittman, R.; Stahelin, R. V.; Wells, C. D., Amot Recognizes a Juxtannuclear Endocytic Recycling Compartment via a Novel Lipid Binding Domain. *Journal of Biological Chemistry* **2010**, 285 (16), 12308-12320.
37. Adler, J. J.; Johnson, D. E.; Heller, B. L.; Bringman, L. R.; Ranahan, W. P.; Conwell, M. D.; Sun, Y.; Hudmon, A.; Wells, C. D., Serum deprivation inhibits the transcriptional co-activator YAP and cell growth via phosphorylation of the 130-kDa isoform of Angiomotin by the LATS1/2 protein kinases. *Proceedings of the National Academy of Sciences* **2013**.
38. Ranahan, W. P.; Han, Z.; Smith-Kinnaman, W.; Nabinger, S. C.; Heller, B.; Herbert, B.-S.; Chan, R.; Wells, C. D., The Adaptor Protein AMOT Promotes the Proliferation of Mammary Epithelial Cells via the Prolonged Activation of the Extracellular Signal-Regulated Kinases. *Cancer Research* **2011**, 71 (6), 2203-2211.
39. Wells, C. D.; Fawcett, J. P.; Traweger, A.; Yamanaka, Y.; Goudreault, M.; Elder, K.; Kulkarni, S.; Gish, G.; Virag, C.; Lim, C.; Colwill, K.; Starostine, A.; Metalnikov, P.; Pawson, T., A Rich1/Amot Complex Regulates the Cdc42 GTPase and Apical-Polarity Proteins in Epithelial Cells. *Cell* **2006**, 125 (3), 535-548.
40. Wells, C. D.; Fawcett, J. P.; Traweger, A.; Yamanaka, Y.; Goudreault, M.; Elder, K.; Kulkarni, S.; Gish, G.; Virag, C.; Lim, C.; Colwill, K.; Starostine, A.; Metalnikov, P.; Pawson, T., A Rich1/Amot Complex Regulates the Cdc42 GTPase and Apical-Polarity Proteins in Epithelial Cells. *Cell* **2006**, 125 (3), 535-548.
41. Knodler, A.; Mayinger, P., Analysis of phosphoinositide-binding proteins using liposomes as an affinity matrix. *BioTechniques* **2005**, 38 (6), 858.
42. Peter, B. J.; Kent, H. M.; Mills, I. G.; Vallis, Y.; Butler, P. J. G.; Evans, P. R.; McMahon, H. T., BAR Domains as Sensors of Membrane Curvature: The Amphiphysin BAR Structure. *Science* **2004**, 303 (5657), 495-499.
43. Gallop, J. L.; Jao, C. C.; Kent, H. M.; Butler, P. J. G.; Evans, P. R.; Langen, R.; McMahon, H. T., Mechanism of endophilin N-BAR domain-mediated membrane curvature. *The EMBO Journal* **2006**, 25 (12), 2898-2910.
44. Mattila, P. K.; Pykäläinen, A.; Saarikangas, J.; Paavilainen, V. O.; Vihinen, H.; Jokitalo, E.; Lappalainen, P., Missing-in-metastasis and IRSp53 deform PI(4,5)P₂-rich membranes by an inverse BAR domain-like mechanism. *The Journal of Cell Biology* **2007**, 176 (7), 953-964.
45. Henne, W. M.; Kent, H. M.; Ford, M. G. J.; Hegde, B. G.; Daumke, O.; Butler, P. J. G.; Mittal, R.; Langen, R.; Evans, P. R.; McMahon, H. T., Structure and Analysis of FCHo2 F-BAR Domain: A Dimerizing and Membrane Recruitment Module that Effects Membrane Curvature. *Structure* **2007**, 15 (7), 839-852.
46. Hillert, M., *Phase equilibria, phase diagrams, and phase transformations: their thermodynamic basis*. Cambridge University Press: 1998.
47. Bancroft, W. D., The Phase Rule in Colloid Chemistry. *The Journal of Physical Chemistry* **1936**, 40 (1), 43-45.
48. Gordon, V. D.; Beales, P. A.; Zhao, Z.; Blake, C.; MacKintosh, F. C.; Olmsted, P. D.; Cates, M. E.; Egelhaaf, S. U.; Poon, W. C. K., Lipid organization and the morphology of solid-like domains in phase-separating binary lipid membranes. *Journal of Physics: Condensed Matter* **2006**, 18 (32), L415.
49. Blosser, Matthew C.; Starr, Jordan B.; Turtle, Cameron W.; Ashcraft, J.; Keller, Sarah L., Minimal Effect of Lipid Charge on Membrane Miscibility Phase Behavior in Three Ternary Systems. *Biophysical Journal* **2013**, 104 (12), 2629-2638.

50. Shimokawa, N.; Hishida, M.; Seto, H.; Yoshikawa, K., Phase separation of a mixture of charged and neutral lipids on a giant vesicle induced by small cations. *Chemical Physics Letters* **2010**, *496* (1), 59-63.
51. Redfern, D. A.; Gericke, A., pH-dependent domain formation in phosphatidylinositol polyphosphate/phosphatidylcholine mixed vesicles. *Journal of Lipid Research* **2005**, *46* (3), 504-515.
52. Redfern, D. A.; Gericke, A., Domain Formation in Phosphatidylinositol Monophosphate/Phosphatidylcholine Mixed Vesicles. *Biophysical Journal* **2004**, *86* (5), 2980-2992.
53. Graber, Z. T.; Gericke, A.; Kooijman, E. E., Phosphatidylinositol-4,5-bisphosphate ionization in the presence of cholesterol, calcium or magnesium ions. *Chemistry and Physics of Lipids* **2014**, *182*, 62-72.
54. Jiang, Z.; Redfern, R. E.; Isler, Y.; Ross, A. H.; Gericke, A., Cholesterol stabilizes fluid phosphoinositide domains. *Chemistry and Physics of Lipids* **2014**, *182*, 52-61.
55. Sarmento, M. J.; Coutinho, A.; Fedorov, A.; Prieto, M.; Fernandes, F., Membrane Order Is a Key Regulator of Divalent Cation-Induced Clustering of PI(3,5)P₂ and PI(4,5)P₂. *Langmuir* **2017**, *33* (43), 12463-12477.
56. Kooijman, E. E.; King, K. E.; Gangoda, M.; Gericke, A., Ionization Properties of Phosphatidylinositol Polyphosphates in Mixed Model Membranes. *Biochemistry* **2009**, *48* (40), 9360-9371.
57. Graber, Z. T.; Jiang, Z.; Gericke, A.; Kooijman, E. E., Phosphatidylinositol-4,5-bisphosphate ionization and domain formation in the presence of lipids with hydrogen bond donor capabilities. *Chemistry and Physics of Lipids* **2012**, *165* (6), 696-704.
58. Graber, Z. T.; Thomas, J.; Johnson, E.; Gericke, A.; Kooijman, E. E., Effect of H-Bond Donor Lipids on Phosphatidylinositol-3,4,5-Trisphosphate Ionization and Clustering. *Biophysical Journal* **2018**, *114* (1), 126-136.
59. Demé, B.; Dubois, M.; Gulik-Krzywicki, T.; Zemb, T., Giant Collective Fluctuations of Charged Membranes at the Lamellar-to-Vesicle Unbinding Transition. 1. Characterization of a New Lipid Morphology by SANS, SAXS, and Electron Microscopy. *Langmuir* **2001**, *18* (4), 997-1004.
60. Colwill, K.; Wells, C. D.; Elder, K.; Goudreault, M.; Hersi, K.; Kulkarni, S.; Hardy, W. R.; Pawson, T.; Morin, G. B., Modification of the Creator recombination system for proteomics applications—improved expression by addition of splice sites. *BMC biotechnology* **2006**, *6* (1), 13.
61. Cha, R.; Tilly, W., *PCR primer*. Cold Spring Harbor Laboratory, Cold Spring Harbor, NY: 1995.
62. Flaman, J.-M.; Frebourg, T.; Moreau, V.; Charbonnier, F.; Martin, C.; Ishioka, C.; Friend, S. H.; Iggo, R., A rapid PCR fidelity assay. *Nucleic acids research* **1994**, *22* (15), 3259.
63. Lundberg, K. S.; Shoemaker, D. D.; Adams, M. W. W.; Short, J. M.; Sorge, J. A.; Mathur, E. J., High-fidelity amplification using a thermostable DNA polymerase isolated from *Pyrococcus furiosus*. *Gene* **1991**, *108* (1), 1-6.
64. Shugar, D., The measurement of lysozyme activity and the ultra-violet inactivation of lysozyme. *Biochimica et Biophysica Acta* **1952**, *8* (0), 302-309.
65. Petrosyan, A.; Ali, M. F.; Verma, S. K.; Cheng, H.; Cheng, P.-W., Non-muscle myosin IIA transports a Golgi glycosyltransferase to the endoplasmic reticulum by binding to its

- cytoplasmic tail. *The International Journal of Biochemistry & Cell Biology* **2012**, *44* (7), 1153-1165.
66. Ali, M. F.; Chachadi, V. B.; Petrosyan, A.; Cheng, P.-W., Golgi Phosphoprotein 3 Determines Cell Binding Properties under Dynamic Flow by Controlling Golgi Localization of Core 2 N-Acetylglucosaminyltransferase 1. *Journal of Biological Chemistry* **2012**, *287* (47), 39564-39577.
67. Bobba, S.; Ponnaluri, V. K. C.; Mukherji, M.; Gutheil, W. G., Microtiter Plate-Based Assay for Inhibitors of Penicillin-Binding Protein 2a from Methicillin-Resistant *Staphylococcus aureus*. *Antimicrobial Agents and Chemotherapy* **2011**, *55* (6), 2783-2787.
68. Koerner, Megan M.; Palacio, Luis A.; Wright, Johnnie W.; Schweitzer, Kelly S.; Ray, Bruce D.; Petrache, Horia I., Electrodynamics of Lipid Membrane Interactions in the Presence of Zwitterionic Buffers. *Biophysical Journal* **2011**, *101* (2), 362-369.
69. Szoka Jr, F.; Papahadjopoulos, D., Comparative properties and methods of preparation of lipid vesicles (liposomes). *Annual review of biophysics and bioengineering* **1980**, *9* (1), 467-508.
70. Woodle, M. C.; Papahadjopoulos, D., [9] Liposome preparation and size characterization. In *Methods in Enzymology*, Sidney Fleischer, B. F., Ed. Academic Press: 1989; Vol. Volume 171, pp 193-217.
71. Schroeder, R.; London, E.; Brown, D., Interactions between saturated acyl chains confer detergent resistance on lipids and glycosylphosphatidylinositol (GPI)-anchored proteins: GPI-anchored proteins in liposomes and cells show similar behavior. *Proceedings of the National Academy of Sciences* **1994**, *91* (25), 12130-12134.
72. Matsuzaki, K.; Murase, O.; Sugishita, K. i.; Yoneyama, S.; Akada, K. y.; Ueha, M.; Nakamura, A.; Kobayashi, S., Optical characterization of liposomes by right angle light scattering and turbidity measurement. *Biochimica et Biophysica Acta (BBA) - Biomembranes* **2000**, *1467* (1), 219-226.
73. Kitamura, A.; Kiyota, T.; Tomohiro, M.; Umeda, A.; Lee, S.; Inoue, T.; Sugihara, G., Morphological Behavior of Acidic and Neutral Liposomes Induced by Basic Amphiphilic α -Helical Peptides with Systematically Varied Hydrophobic-Hydrophilic Balance. *Biophysical Journal* **1999**, *76* (3), 1457-1468.
74. Ilavsky, J.; Jemian, P. R., Irena: tool suite for modeling and analysis of small-angle scattering. *Journal of Applied Crystallography* **2009**, *42* (2), 347-353.
75. Nagle, J. F.; Wiener, M. C., Structure of fully hydrated bilayer dispersions. *BBA - Biomembranes* **1988**, *942* (1), 1-10.
76. Rand, R.; Fuller, N.; Parsegian, V.; Rau, D., Variation in hydration forces between neutral phospholipid bilayers: evidence for hydration attraction. *Biochemistry* **1988**, *27* (20), 7711.
77. Helm, C. A.; Tippmann-Krayer, P.; Möhwald, H.; Als-Nielsen, J.; Kjaer, K., Phases of phosphatidyl ethanolamine monolayers studied by synchrotron x-ray scattering. *Biophysical Journal* **1991**, *60* (6), 1457-1476.
78. Rappolt, M.; Hickel, A.; Bringezu, F.; Lohner, K., Mechanism of the Lamellar/Inverse Hexagonal Phase Transition Examined by High Resolution X-Ray Diffraction. *Biophysical Journal* **2003**, *84* (5), 3111-3122.
79. Johnson, M. A.; Seifert, S.; Petrache, H. I.; Kimble-Hill, A. C., Phase Coexistence in Single-Lipid Membranes Induced by Buffering Agents. *Langmuir* **2014**, *30* (33), 9880-9885.
80. Filippov, A.; Orädd, G.; Lindblom, G., The Effect of Cholesterol on the Lateral Diffusion of Phospholipids in Oriented Bilayers. *Biophys J* **2003**, *84*, 3079-3086.

81. Scherfeld, D.; Kahya, N.; Schwille, P., Lipid Dynamics and Domain Formation in Model Membranes Composed of Ternary Mixtures of Unsaturated and Saturated Phosphatidylcholines and Cholesterol. *Biophysical J.* **2003**, *85*, 3758-3768.
82. Veatch, S. L.; Keller, S. L., Separation of Liquid Phases in Giant Vesicles of Ternary Mixtures of Phospholipids and Cholesterol. *Biophysical Journal* **2003**, *85* (5), 3074-3083.
83. Crane, J. M.; Tamm, L.K., Role of Cholesterol in the Formation and Nature of Lipid Rafts in Planar and Spherical Model Membranes. *Biophysical J* **2004**, *86*, 2965-2979.
84. Stottrup, B. L.; Stevens, D. S.; Keller, S. L., Miscibility of Ternary Mixtures of Phospholipids and Cholesterol in Monolayers, and Application to Bilayer Systems. *Biophys J* **2005**, *88* (1), 269-276.
85. Veatch, S. L.; Keller, S. L., Seeing spots: Complex phase behavior in simple membranes. *Biochimica et Biophysica Acta (BBA) - Molecular Cell Research* **2005**, *1746* (3), 172-185.
86. Pathak, P.; London, E., Measurement of Lipid Nanodomain (Raft) Formation and Size in Sphingomyelin/POPC/Cholesterol Vesicles Shows TX-100 and Transmembrane Helices Increase Domain Size by Coalescing Preexisting Nanodomains But Do Not Induce Domain Formation. *Biophysical Journal* **2011**, *101* (10), 2417-2425.
87. Pathak, P.; London, E., The Effect of Membrane Lipid Composition on the Formation of Lipid Ultrananodomains. *Biophysical Journal* **2015**, *109* (8), 1630-1638.
88. Neves, A. R.; Nunes, C.; Reis, S., Resveratrol induces ordered domains formation in biomembranes: Implication for its pleiotropic action. *Biochimica et Biophysica Acta - Biomembranes* **2016**, *1858* (1), 12-18.
89. Huang, Z.; Toledo, A. M.; Benach, J. L.; London, E., Ordered Membrane Domain-Forming Properties of the Lipids of *Borrelia burgdorferi*. *Biophysical Journal* **2016**, *111* (12), 2666-2675.
90. Suga, K.; Akizaki, K.; Umakoshi, H., Quantitative Monitoring of Microphase Separation Behaviors in Cationic Liposomes Using HHC, DPH, and Laurdan: Estimation of the Local Electrostatic Potentials in Microdomains. *Langmuir* **2016**, *32* (15), 3630-3636.
91. Dietrich, C.; Bagatolli, L. A.; Volovyk, Z. N.; Thompson, N. L.; Levi, M.; Jacobson, K.; Gratton, E., Lipid Rafts Reconstituted in Model Membranes. *Biophys J* **2001**, *80* (3), 1417-1428.
92. Canham, P. B., The minimum energy of bending as a possible explanation of the biconcave shape of the human red blood cell. *Journal of Theoretical Biology* **1970**, *26* (1), 61-81.
93. Mukherjee, S.; Maxfield, F. R., Role of Membrane Organization and Membrane Domains in Endocytic Lipid Trafficking. *Traffic* **2000**, *1* (3), 203-211.
94. Tian, A.; Baumgart, T., Sorting of Lipids and Proteins in Membrane Curvature Gradients. *Biophysical Journal* **2009**, *96* (7), 2676-2688.
95. Maxfield, F. R.; McGraw, T. E., Endocytic recycling. *Nat Rev Mol Cell Biol* **2004**, *5* (2), 121-132.
96. Meer, G. v.; Sprong, H., Membrane lipids and vesicular traffic. *Current Opinion in Cell Biology* **2004**, *16* (4), 373-378.
97. van Meer, G.; Voelker, D. R.; Feigenson, G. W., Membrane lipids: where they are and how they behave. *Nat Rev Mol Cell Biol* **2008**, *9* (2), 112-124.
98. Janmey, P. A.; Kinnunen, P. K. J., Biophysical properties of lipids and dynamic membranes. *Trends in Cell Biology* **2006**, *16* (10), 538-546.
99. Suetsugu, S.; Kurisu, S.; Takenawa, T., Dynamic Shaping of Cellular Membranes by Phospholipids and Membrane-Deforming Proteins. *Physiological Reviews* **2014**, *94* (4), 1219-1248.

1
2
3 100. Israelachvili, J., *Intermolecular and Surface Forces* Cambridge University Press,
4 Cambridge: Academic, London, 1991.

5 101. Kamal, M. M.; Mills, D.; Grzybek, M.; Howard, J., Measurement of the membrane
6 curvature preference of phospholipids reveals only weak coupling between lipid shape and
7 leaflet curvature. *Proceedings of the National Academy of Sciences* **2009**, *106* (52), 22245-
8 22250.
9
10
11
12
13
14
15
16
17
18
19
20
21
22
23
24
25
26
27
28
29
30
31
32
33
34
35
36
37
38
39
40
41
42
43
44
45
46
47
48
49
50
51
52
53
54
55
56
57
58
59
60

TOC Graphic

